Enhancing Dynamic Voltage Stability in Power Systems with Distributed Generations

Qitao Liu, Hongjian Sun, and Peter Matthews

Department of Engineering, Durham University, Durham, UK
Email: {qitao.liu, hongjian.sun, p.c.matthews}@durham.ac.uk

***Abstract*—Voltage stability is critical in the power distribution network. This paper aims to study the dynamic voltage stability problem. When wind generators reach maximum reactive power output, the bus voltage will operate near its steady-state stability limit. In order to avoid voltage instability, a dynamic L-index minimization approach is proposed by incorporating both wind generators and other reactive power resources. It then verifies the proposed voltage stability enhancement method using real load and wind generation data in the IEEE 14 bus system. The simulation results show the benefits of proposed methodology in solving dynamic-state voltage stability enhancement problem.**

***Index Terms*—dynamic-state, loadability margin, PV curves, reactive power, voltage stability.**

I. Introduction

Voltage instability is a major problem of power systems. It has caused several incidences in different countries, for example, the blackouts in Ohio, Michigan, New York and Ontario on August 14, 2003 [1]. These contingencies and voltage collapses have prompted that a significant effort should be made towards the study and prevention of voltage instabilities.

In recent years, there is a trend of high penetration of renewable energy in the traditional power grid. Meanwhile, load characteristics have a significant impact on power system behaviours [2]. Both load and distributed generations (DGs) should be taken into account when voltage stability problems are considered. A load model is a mathematical representation of the relationship between voltage magnitude and the power at a bus [3]. It was assumed that loads are constant and increased in proportion for loadability computation [4]. Load composition model was proposed in [5], where loads were modelled as a combination of constant power, constant current and constant impedance. Additionally, generators were normally modelled as either PV buses or ideal voltage sources. L-index was extended to incorporate generator equivalent model for voltage stability analysis [6]. In the generator equivalent model, generators were modelled by internal voltages and impedances to capture the dynamic behaviours of generators.

Several methodologies for voltage stability analysis, such as Power-Voltage (PV) curves based indices [7], Jacobian matrix singularity [8], L-index [9] were proposed. These metrics can reflect the voltage stability condition if the voltage is stable for a given operating condition. Besides, PV curves also show the distance for the system between its current operating point and voltage stability limit. The impacts of variations in reactive power output of Doubly Fed Induction Generators (DFIGs) on the voltage stability of systems were studied in many papers. Wu $et\ al.$ [10] presented a decoupled control technique for active and reactive power of DFIGs and it was widely used in the control design of wind generators with DFIGs. It was suggested that system dynamics could be dramatically improved through an appropriate control strategy with reactive power compensators [11]. Han $et\ al.$ [12] studied static synchronous compensator (STATCOM) and its impact on the integration of a large wind farm into a weak power system. It was shown that voltage fluctuation could be affected by the size and location of the STATCOM. Different approaches were proposed to improve the voltage stability margin. A singular value sensitivity based optimal control for steady-State voltage stability enhancement was proposed in [13]. Xu $et\ al.$ [14] presented an approach of optimal placement of static compensators for multi-objective voltage stability enhancement.

In summary, aforesaid approaches studied the impacts of DG units on the voltage stability. Their impacts on the voltage stability were studied by considering the variations in reactive power output of variable-speed wind generators and reactive power compensators. It was shown that significant improvement in the voltage stability margin could be obtained with proper coordination controls [15]. Moreover, some dynamic loads models and wind generations models were taken into account for dynamic voltage stability analysis. However, little work has been done on the voltage stability enhancement using dynamic load data and dynamic wind generation data. Different from existing works, the objective of this paper is to study the dynamic voltage stability enhancement problem with dynamic loads and wind generations.

The main contributions of this paper are:

- It presents a dynamic voltage stability enhancement method by coordinating the reactive power sources. Both wind generators and additional installed static VAR compensators (SVCs) are taken into account based on IEEE 14 bus system.
- Real data (from both wind generations and loads) for 24 hours and 1 year are applied in the proposed method for time-series simulations.
- Benefits on enhancing system loadability are analysed. The effect of variations in the wind generation and demand on the loadability is investigated.

This paper is organized as follows. In Section II, system model and analysis tool are presented. Section III shows the proposed methodology for voltage stability enhancement. Section IV verifies the proposed method using IEEE 14 bus systems together with real dynamic load and wind generation data. Conclusions are given in Section VI.

II. Relationship Between Voltage and Power

Voltage stability is an important measure in power system operations. It depends on the system status, such as the load bus voltage magnitude, the power transmission, the reactive power injection and absorption. In this section, both mathematical expression and figures are used to illustrate the relationship between voltage and power.

A. Mathematical Expression

Newton Raphson method has been widely used in power-flow study [16], which can be given by

$$\begin{bmatrix}\Delta P\\ \Delta Q\end{bmatrix} = J\begin{bmatrix}\Delta\theta\\ \Delta\left|V\right|\end{bmatrix}. \tag{1}$$

where ΔP and ΔQ are the mismatch equations, and are given in (2) and (3) below

$$\Delta P = -P_e + \sum_{f=1}^{N} |V_e|\,|V_f|\,(G_{ef}\cos\theta_{ef} + B_{ef}\sin\theta_{ef}). \tag{2}$$

$$\Delta Q = -Q_e + \sum_{f=1}^{N} |V_e|\,|V_f|\,(G_{ef}\sin\theta_{ef} - B_{ef}\cos\theta_{ef}). \tag{3}$$

where P_e is the net power injected at the bus e, Q_e is the net reactive power injected at the bus e. V_e and V_f are the voltage at bus e and f, respectively. G_{ef} is the real part of the element in Y_{bus} corresponding to the eth row and fth column, B_{ef} is the imaginary part of the element in Y_{bus} corresponding to the eth row and fth column and θ_{ef} is the difference in voltage angle between the eth and fth buses ($\theta_{ef} = \delta_e - \delta_f$). J is a matrix of partial derivatives, called as Jacobian matrix as below

$$J = \begin{bmatrix}\frac{\partial\Delta P}{\partial\theta} & \frac{\partial\Delta P}{\partial|V|}\\ \frac{\partial\Delta Q}{\partial\theta} & \frac{\partial\Delta Q}{\partial|V|}\end{bmatrix}. \tag{4}$$

Once the computation of Newton Raphson method is completed, the voltages of both load and generator bus can be determined by using (1) and expressed as V_j and V_i, respectively.

B. PV Curves

P-V curve analysis is used to show the voltage stability of power system and determine the voltage collapse point. For this analysis, active power of the load at a particular bus is increased in steps and voltage is then observed. Curves for those particular buses will be plotted based on the continuous power flow (CPF) to determine the voltage stability of a system.

CPF can be used to trace the power flow solution, begins with a base load and obtains the maximum transfer power by increasing load. Thus the loadability margin can be obtained which is the maximum active load at the critical bus in the power system.

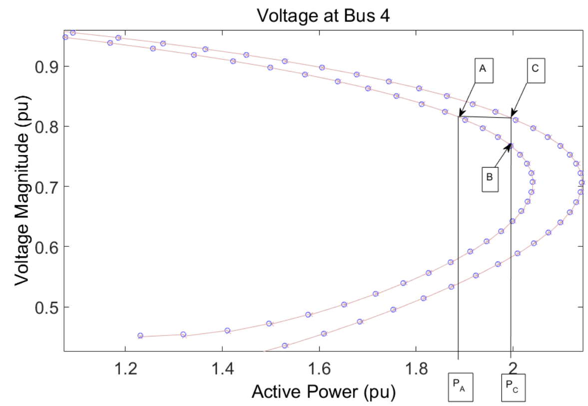

Fig. 1. PV curves in the presence of an SVC

Fig. 1 shows the PV characteristic when the network has a SVC. It is assumed that the system is operating at the base point A. Meanwhile the load power is increased from P_A to P_C. Without controlling SVC, the new operating point would be at B. This causes a voltage drop which indicates the power cost on the transmission line. From point A to point C, it can be seen that voltage falls slightly with controlling SVC.

III. Methodology

It is known that power demand and supply are affected by weather, season, hour of day, etc. Meanwhile, there is a trend of the high renewable energy penetration in the power system. These varying power demand and supply may worsen the imbalance between demand and supply, which may result in reduced loadability and reach the edge of the voltage stability limit, hence endanger the whole power system. The objective of this paper is to enhance the dynamic voltage stability of power system with distributed generations. L-index is adopted in this paper as an objective for dynamic voltage stability enhancement.

A. Objective Function

Loadability margin is used to indicate how much the maximum power can be transferred through the transmission line based on the stability limits and device constraint. L-index is a linear indicator of voltage stability state of critical load buses. A smaller value of L-index indicates that the voltage is more stable. It is assumed that generators are ideal voltage source and terminal voltages of generators are constants. The calculation of L-index relies on the real-time measurements, which can be obtained from phasor measurement units (PMUs) [17]. The L-index is computed as

$$L_j = \left|1 - \sum_{i=1}^{g} F_{ji}\frac{V_i}{V_j}\right|. \tag{5}$$

where V indicates the voltages at the bus and subscripts j and i are used to differentiate between load and generator bus numbers. $1, ..., g$ are the generators. F_{ji} in (5) is the element of the F_{lg} matrix which is obtained by admittance matrix calculation. The relationship between voltage and current is,

$$\begin{bmatrix} V_l \\ I_g \end{bmatrix} = \begin{bmatrix} Z_{ll} & F_{lg} \\ K_{gl} & Y_{gg} \end{bmatrix} \begin{bmatrix} I_l \\ V_g \end{bmatrix} \tag{6}$$

where F_{lg} is computed as $[F_{lg}] = -[Y_{ll}]^{-1}[Y_{lg}]$. Y_{ll} is the self-admittance at the node l and Y_{lg} is the mutual admittances between the nodes l and g.

The relationship between L-index and loadability is proposed in [18] and verified in [15]. It indicates that a smaller value of L-index can achieve a larger loadability margin. Therefore, L-index is employed in voltage stability enhancement as a measure of loadability. Compared to Jacobian matrix based lowest singular value method, the elements of F_{ji} in the formulation of L-index are usually readily available. Besides, the value of L-index is determined only from voltages at generator and load buses, thus no power flow calculation is required.

To improve the steady-state voltage stability of the power system, the loadability margin at all nodes should be maximized, which in turn minimize the value of L-index for each bus. The objective function thus can be written by

$$T(Q) = \sum_{j=g+1}^{n} L_j^2 \tag{7}$$

where n is the total number of buses in the system.

Reactive power compensation, which is injecting reactive power into the power system, helps to reduce line currents and network losses, so that voltages can be kept close to the nominal values and stability enhanced. Therefore, voltage stability margins can be significantly improved by appropriate reactive power compensation. It is assumed that SVC has been installed on each load bus. Due to the rotor current injection schemes, the reactive power output can also be controlled. Controlling wind generators as the sources of reactive power is feasible. Therefore, the control variables are Q_{svc} and Q_{wg}, which represent the reactive power output of SVCs and wind generators, respectively. The optimization formulation can be defined by combining the objective function and the associated constraints, as follows:

$$\begin{aligned} \min T(Q) = \sum_{j=g+1}^{n} L_j^2 \\ \text{s.t. } Q_{wg}^{min} \le Q_{wg} \le Q_{wg}^{max} \\ Q_{svc}^{min} \le Q_{svc} \le Q_{svc}^{max} \end{aligned} \tag{8}$$

where Q is the control variable including: Q_{svc} and Q_{wg}.

B. Optimisation Algorithm

Trust region algorithm [15] is applied to find the minimum value of the objective function. The limits of control variables are also considered. To implement the trust region, the gradient of the objective function is provided. The derivation process of gradient is shown below:

$$\frac{\partial T(Q)}{\partial V_i} = \frac{\partial}{\partial V_i}\left(\sum_{j=g+1}^{n} L_j^2\right) \tag{9}$$

where the term L_j^2 can be rewritten as

$$L_j^2 = \left[1 - \sum_{i=1}^{g} C_{ji}\frac{V_i}{V_j}\right]^2 + \left[\sum_{i=1}^{g} D_{ji}\frac{V_i}{V_j}\right]^2 \tag{10}$$

in which

$$C_{ji} = F_{ji}\cos(\theta_{ji} + \delta_i - \delta_j) \tag{11}$$

$$D_{ji} = F_{ji}\sin(\theta_{ji} + \delta_i - \delta_j). \tag{12}$$

The partial derivative for $T(Q)$ with respect to V_i and V_j can be given as

$$\frac{\partial L_j^2}{\partial V_i} = 2\left[1 - \sum_{i=1}^{g} C_{ji}\frac{V_i}{V_j}\right]\left[\frac{-C_{ji}}{V_j}\right] + 2\left[\sum_{i=1}^{g} D_{ji}\frac{V_i}{V_j}\right]\left[\frac{D_{ji}}{V_j}\right] \tag{13}$$

$$\begin{aligned} \frac{\partial L_j^2}{\partial V_j} = 2\left[1 - \sum_{i=1}^{g} C_{ji}\frac{V_i}{V_j}\right]\left[\sum_{i=1}^{g} C_{ji}\frac{V_i}{V_j^2}\right] + \\ 2\left[\sum_{i=1}^{g} D_{ji}\frac{V_i}{V_j}\right]\left[-\sum_{i=1}^{g} D_{ji}\frac{V_i}{V_j^2}\right]. \end{aligned} \tag{14}$$

Finally, the partial derivative for $T(Q)$ with respect to reactive power output of various reactive source can be computed as

$$\begin{bmatrix} \frac{\partial T(Q)}{\partial Q_2} \\ \vdots \\ \frac{\partial T(Q)}{\partial Q_n} \end{bmatrix} = \begin{bmatrix} \frac{\partial Q_2}{\partial V_2} & \cdots & \frac{\partial Q_2}{\partial V_n} \\ \vdots & \ddots & \vdots \\ \frac{\partial Q_2}{\partial V_2} & \cdots & \frac{\partial Q_n}{\partial V_n} \end{bmatrix}^{-1} \begin{bmatrix} \frac{\partial T(Q)}{\partial V_2} \\ \vdots \\ \frac{\partial T(Q)}{\partial V_n} \end{bmatrix}. \tag{15}$$

In the optimization, trust region is a local search method that begin with a given solution. In each iteration, a new solution will be created. Trust region determines whether to keep the old solution, or to drop the old one and keep the new one for the next iteration, which means the better of the two will be kept.

IV. Simulation Results

The proposed method is implemented in Matlab using the IEEE 14 bus system. Matpower [19] is used to solve power flow and optimal power flow problems and the tool to draw the PV curves. The base bus system parameters are from case14.m produced by Matpower. For the comparison purpose, there is no control actions in the base condition. Dynamic optimisation means the power of supply and demand vary with time. The control algorithm is implemented in an iterative manner. Once an optimisation is finished with a set of data, the next cycle will start. During each cycle, loadability margin can be achieved at the normal operating condition. With the coordination control of reactive power output of wind generators and other reactive power sources, larger loadability can be achieved. Thus, the voltage stability can be enhanced based on dynamic data.

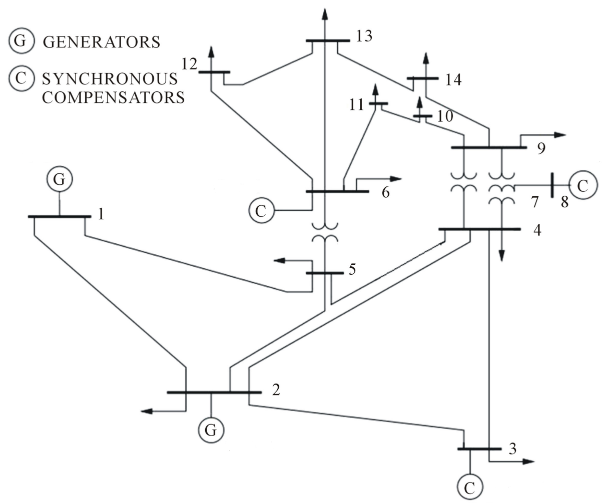

Fig. 2. IEEE 14 bus System [20]

Fig.2 shows the IEEE 14 bus system. It is assumed that generators installed on bus 2 are DFIGs. The wind farm consists of 100 generators, each rated at 2 MW. SVC has been installed on each load bus, each rated at 50 MVAR. This IEEE 14 bus system contains one wind farm on bus 2. Generation and load profiles are obtained from Gridwatch provided by BM reports [21]. The data are for the whole year of 2015. To simplify the calculations, hourly data are extracted from raw generation and load profiles. Then, they can be applied to the proposed method.

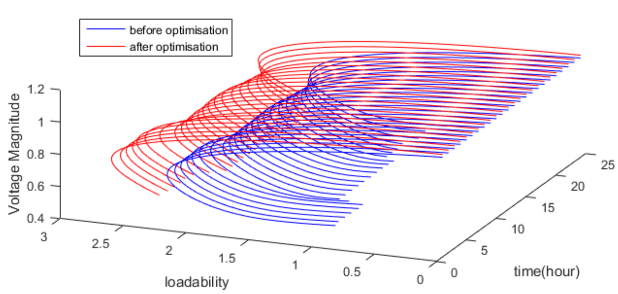

Fig. 3. one day hourly PV curves

In Fig.3, 3D PV curves are given using one whole day (1 May 2015) around load and wind generation data. The PV curves are drawn each hour. Blue lines are normal conditions where no control action is considered. After optimisation by using coordination control, the new PV curves are drawn with red colour. It can be seen that the loadability is enlarged significantly when applied the proposed method. From 10am to 9pm, the loadability margins are relative higher, due to the heavier load compared to the sleeping time.

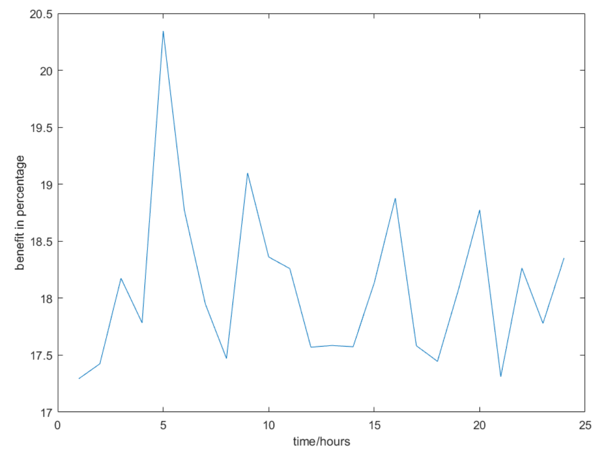

Fig. 4. hourly loadability benefit in percentage

It is also important to know the growth rate of loadability between base condition and after optimisation. With one day real data of wind generation and load, the curve in Fig.4 indicates the one-day hourly benefit from using the proposed method. The curve is plotted from 1am to midnight. It can be seen that there are some fluctuations. Higher benefits occur at 6am, 9am, 4pm and 8pm. The highest benefit value is 20.3% at 6 am and the lowest value is 17.3% at 1am. Due to the loads are at the same level in the night and in the early morning, wind generation determines benefits. Higher wind generation helps achieve higher benefit.

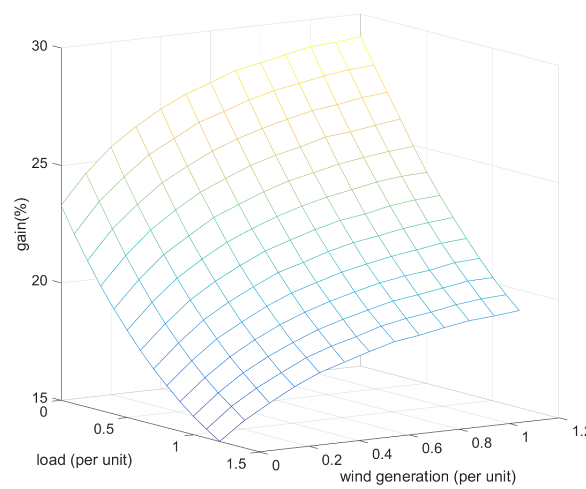

Fig. 5. loadability benefit based on different wind generation and demand.

The benefits of different wind generation and demand are plotted in 3-dimension shown in Fig.5. It can be seen that with the increasing of demand, the benefit is decreased. On the other hand, it is noted that loadability is enlarged when wind energy is integrated into power system. Therefore, the integration of wind energy has a positive effect on the power system. Fig.5 also shows highest value of benefit, i.e. around 28%. In this case, it is caused by higher wind generation and lower demand. The lowest value (15%) of benefit occurs, when the system has heavier load and without wind generation.

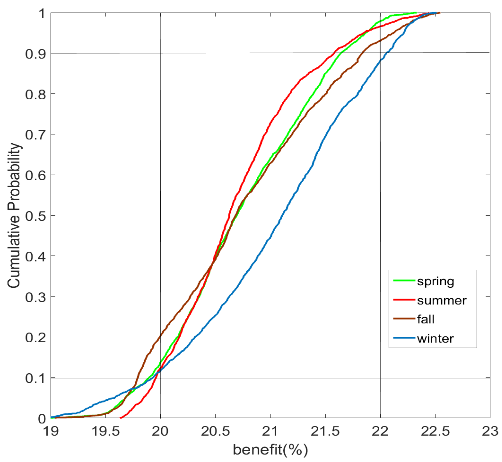

Fig. 6. comparison of four seasons loadability benefit based on cumulative distribution functions.

Fig. 6 displays benefits analysis based on cumulative distribution functions for four seasons in one year based on UK annual data. The Cumulative Distribution Function indicates the probability of a random variate less than or equal to a certain value. It can be seen that the cumulative probability of red line is always larger than other lines', when the benefit is larger than 20.5%. Thus, the proposed method has the best performance in summer. The heaviest load and lower wind generation in winter, will caused the worst performance. It is observed that 80% of the data based on one year loadability benefit are distributed in the region of 20% to 22%. Hence the performance of proposed approach is stable.

V. Conclusion

A dynamic voltage stability enhancement method is presented. It is proved that it is feasible to enhance the voltage stability with proper coordination control of reactive power output of wind generators and other reactive controllers under dynamic conditions. The L-index based voltage stability control method is verified in the IEEE 14 bus system. The benefits of optimisation based on different wind generation and demand are illustrated. Further, loadability benefits in four seasons are compared. This proposed method can be easily extended to other different power networks where the power system is integrated with wind farms.

Acknowledgments

This work was supported by the EPSRC (grant EP/P005950/1); and the European commissions horizon 2020 framework programme (H2020/2014-2020) under grant agreement No. 734325 testbed project.

References

[1] G. Andersson, P. Donalek, R. Farmer, and N. Hatziargyriou, "Causes of the 2003 major grid blackouts in north america and europe, and recommended means to improve system dynamic performance," *IEEE Transactions on Power Systems*, vol. 20, no. 4, pp. 1922–1928, Nov 2005.

[2] A. Rouhani and A. Abur, "Real-time dynamic parameter estimation for an exponential dynamic load model," *IEEE Transactions on Smart Grid*, vol. 7, no. 3, pp. 1530–1536, May 2016.

[3] "Load representation for dynamic performance analysis of power systems," *IEEE Transactions on Power Systems*, vol. 8, no. 2, pp. 472–482, May 1993.

[4] Q. Y. Liu, C. C. Liu, and Q. F. Liu, "Coordinated voltage control with online energy margin constraints," *IEEE Transactions on Power Systems*, vol. 31, no. 3, pp. 2064–2075, May 2016.

[5] K. Morison, H. Hamadani, and L. Wang, "Practical issues in load modeling for voltage stability studies," in *Proc. IEEE PES General Meeting*, vol. 3, July 2003, pp. 1392–1397 Vol. 3.

[6] Y. Wang, C. Wang, F. Lin, W. Li, L. Y. Wang, and J. Zhao, "Incorporating generator equivalent model into voltage stability analysis," *IEEE Transactions on Power Systems*, vol. 28, no. 4, pp. 4857–4866, Nov 2013.

[7] V. Ajjarapu and C. Christy, "The continuation power flow: a tool for steady state voltage stability analysis," *IEEE Transactions on Power Systems*, vol. 7, no. 1, pp. 416–423, Feb 1992.

[8] P.-A. Lof, T. Smed, G. Andersson, and D. Hill, "Fast calculation of a voltage stability index," *IEEE Transactions on Power Systems*, vol. 7, no. 1, pp. 54–64, Feb 1992.

[9] B. Gao, G. Morison, and P. Kundur, "Voltage stability evaluation using modal analysis," *IEEE Transactions on Power Systems*, vol. 7, no. 4, pp. 1529–1542, Nov 1992.

[10] F. Wu, X.-P. Zhang, P. Ju, and M. Sterling, "Decentralized nonlinear control of wind turbine with doubly fed induction generator," *IEEE Transactions on Power Systems*, vol. 23, no. 2, pp. 613–621, May 2008.

[11] M. El Moursi, B. Bak-Jensen, and M. Abdel-Rahman, "Coordinated voltage control scheme for seig-based wind park utilizing substation statcom and ultc transformer," *IEEE Transactions on Sustainable Energy*, vol. 2, no. 3, pp. 246–255, Jul 2011.

[12] C. Han, A. Q. Huang, M. E. Baran, S. Bhattacharya, W. Litzenberger, L. Anderson, A. L. Johnson, and A. A. Edris, "Statcom impact study on the integration of a large wind farm into a weak loop power system," *IEEE Transactions on Energy Conversion*, vol. 23, no. 1, pp. 226–233, Mar 2008.

[13] O. A. Urquidez and L. Xie, "Singular value sensitivity based optimal control of embedded VSC-HVDC for steady-state voltage stability enhancement," *IEEE Transactions on Power Systems*, vol. 31, no. 1, pp. 216–225, Jan 2016.

[14] Y. Xu, Z. Y. Dong, C. Xiao, R. Zhang, and K. P. Wong, "Optimal placement of static compensators for multi-objective voltage stability enhancement of power systems," *IET Generation, Transmission Distribution*, vol. 9, no. 15, pp. 2144–2151, 2015.

[15] V. Kumar, K. Reddy, and D. Thukaram, "Coordination of reactive power in grid-connected wind farms for voltage stability enhancement," *IEEE Transactions on Power Systems*, vol. 29, no. 5, pp. 2381–2390, Sept 2014.

[16] H. L. Nguyen, "Newton-raphson method in complex form [power system load flow analysis]," *IEEE Transactions on Power Systems*, vol. 12, no. 3, pp. 1355–1359, Aug 1997.

[17] P. Yang, Z. Tan, A. Wiesel, and A. Nehora, "Power system state estimation using pmus with imperfect synchronization," *IEEE Transactions on Power Systems*, vol. 28, no. 4, pp. 4162–4172, Nov 2013.

[18] P. Kessel and H. Glavitsch, "Estimating the voltage stability of a power system," *IEEE Transactions on Power Delivery*, vol. 1, no. 3, pp. 346–354, July 1986.

[19] C. E. M.-S. Ray D. Zimmerman, *Power Systems Engineering Research Center (PSERC)*, Available: http://www.pserc.cornell.edu/matpower/.

[20] R. Christie, *UW Power System Test Case Archive*, Available: http://www.ee.washington.edu/research/pstca/.

[21] National Grid Status. Available: http://www.gridwatch.templar.co.uk/.